Particle Accelerators, 1988, Vol. 22, pp. 273–299
Reprints available directly from the publisher
Photocopying permitted by license only

Printed in the United States of America

STUDY OF ALTERNATING-PERIODIC-STRUCTURE CAVITIES WITH A DISK-LOADED WAVEGUIDE MODEL

Y. YAMAZAKI, T. HIGO, and K. TAKATA
National Laboratory for High Energy Physics, Oho-machi, Tsukuba-gun, Ibaraki-ken, 305, Japan

(Received December 22, 1986)

An alternating periodic structure (APS) electrically coupled through beam apertures was studied by developing a disk-loaded waveguide model. Results of the model calculation are in good agreement with those of the SUPERFISH calculation for the case of a two-cell APS cavity. Fields in coupling cells were excited by differences among accelerating cell frequencies, resulting in a decrease in the Q-value. If the confluent condition is not satisfied, that is, if a stopband appears, the energy is stored nonuniformly among the accelerating cells with different accelerating frequencies. In this case the coupling-mode frequency should be higher than the accelerating-mode frequency to stabilize the field distribution.

1. INTRODUCTION

It is well known that accelerating cavities with an alternating periodic structure (APS)[1–6] have the excellent field stability of the $\pi/2$ mode, while keeping the high shunt impedance of the π mode. Therefore, the APS with nine electrically coupled accelerating cells[7,8] shown in Fig. 1 and Table I was chosen for 508-MHz rf accelerating cavities in the TRISTAN main ring. To maximize the shunt impedance for the given structure it is preferable to minimize the length l_c of the coupling cell, since it does not accelerate the beam. Thus, the length l_c of the coupling cell was first proposed to be 15 mm, the smallest practical value. (The rationale for this choice is detailed in Ref. 7.)

Actual APS cavities will deviate from the ideally periodic structure, and knowledge about the effect of the deviation is necessary for practical design. In particular, the TRISTAN cavities will have large frequency shifts due to thermal expansion, since they are operated with a high-power continuous wave (more than 150 kW). Consequently, a large deviation from the ideal periodicity is expected, unless all of the cells including coupling cells are tuned to the same rf frequency with sophisticated and complicated tuning devices.

Characteristics of APS cavities have been studied by many authors (see Refs. 1–6 and references therein), and the effect of the deviation has been discussed in some of the articles. However, only relatively small deviations have been taken into account, and the effect of the deviation on the small coupling cells is not seriously considered. Thus, the purpose of the present study is to investigate the effect of the large deviation from the ideal periodicity on an APS cavity with very small coupling cells.

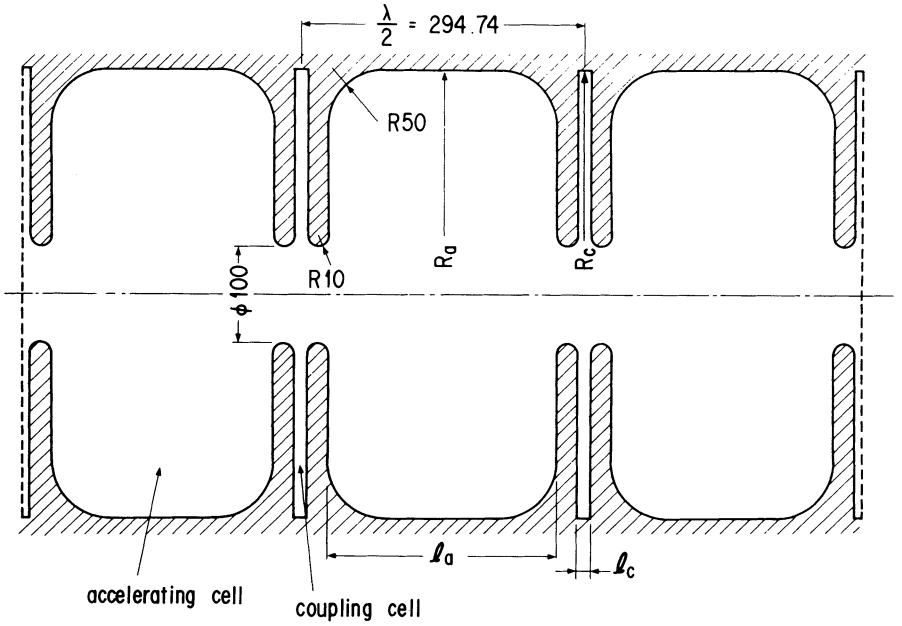

FIGURE 1 Alternating periodic structure electrically coupled through the beam aperture.

For this purpose calculation with the computer program SUPERFISH[9] would be most reliable, if the cavity consisted of a few cells. However, as the number of the cells are increased up to nine, as in the present case, SUPERFISH requires excessive computing time or too much memory area, or both, for available computers to calculate the various parameters with the necessary accuracy. Therefore, a simple model suitable for the present purpose must be chosen among the possible candidates.

A coupled-resonator model developed by Nagle *et al.*[3,4] is one candidate. It has been used for the study of the side-coupled cavity chain. However, equations of

TABLE I
Parameters of the APS Cavities

	SUPERFISH	Model	SUPERFISH
l_c (mm)	15.00	15.00	30.00
l_a (mm)	224.74	246.00	209.74
f_c (MHz)	508.58	508.58	508.58
f_a (MHz)	508.58	508.58	508.58
R_c (mm)	238.45	230.43	235.20
R_a (mm)	321.91	225.90	232.28
b	—	0.01411	—
Q_c	4,830	—	9,083
Q_a	43,830	—	42,450
R_{sh} ($M\Omega/m$)	27.3	—	26.7

the model were derived from a circuit analog of a chain of magnetically coupled circuits, and, consequently, the correspondence between the parameters of the coupled-resonator model and those of a chain of the electrically coupled cells is not obvious. Furthermore, validity of the model calculation is not quantitatively guaranteed for the effect of the *large* deviation from the ideal periodicity, particularly in the case of the very small coupling cells.

Thus, a disk-loaded waveguide model[10] was developed to simulate the cavity with electrically coupled cells. The model is so simple that a small microcomputer can be used to calculate a resonant frequency and Q-value of multicell cavities for many varieties of parameters. Also, the correspondence between parameters of the model and of the electrically coupled multicell cavity is straightforward. Thus, it is easy to interpret the meaning of the model parameters.

In the next section, the disk-loaded waveguide model is described in detail. Then, in Section 3, the model is applied to an ideally periodic APS cavity, and some characteristics of the APS cavity are discussed. In Section 4 a two-cell APS cavity is studied with the model calculation and SUPERFISH calculation. Here, the accuracy of the model calculation is examined by comparing results of the two calculations. In Section 5 the disk-loaded waveguide model is used to study the effect of the deviation from the ideal periodicity in the nine-cell APS cavity. In Section 6 the results of the calculation are discussed, and the APS cavity with the larger coupling-cell gap length is proposed for the TRISTAN main ring.

2. DISK-LOADED CYLINDRICAL-WAVEGUIDE MODEL

In a disk-loaded cylindrical-waveguide model, the nth cell is coupled with the $(n+1)$-th cell through a small circular iris, as shown in Fig. 2. Electromagnetic fields in a waveguide are well described in terms of a voltage and current in a transmission line. In particular the voltage and current are proportional to the

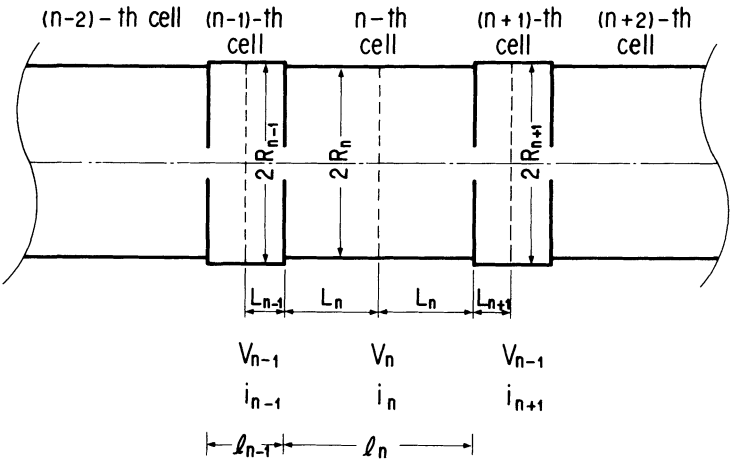

FIGURE 2 Disk-loaded cylindrical waveguide.

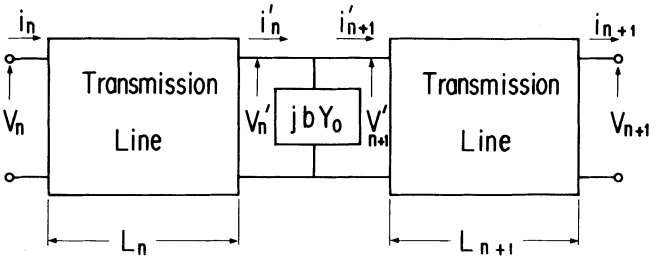

FIGURE 3 Equivalent circuit of the disk-loaded cylindrical waveguide.

radial electric field E_r and aximuthal magnetic field H_ϕ, respectively, of a TM01 mode at the surface of the waveguide. The effect of the iris on the fields of the TM01 mode is well represented by that of shunt susceptance jbY_0 on the voltage and current, as shown in Fig. 3, where Y_0 is a characteristic admittance of the vacuum.

The voltage V_n and current i_n at the center of the nth cell are transformed to V_{n+1} and i_{n+1} of the $(n+1)$-th cell as

$$\begin{pmatrix} V_{n+1} \\ i_{n+1} \end{pmatrix} = \begin{pmatrix} t_{11}^{(n)} & t_{12}^{(n)} \\ t_{21}^{(n)} & t_{22}^{(n)} \end{pmatrix} \begin{pmatrix} V_n \\ i_n \end{pmatrix} = [t^{(n)}] \begin{pmatrix} V_n \\ i_n \end{pmatrix}. \tag{1}$$

The transformation matrix $[t^{(n)}]$ for the lossless disk-loaded waveguide is a function of a frequency f and includes R_n, R_{n+1}, L_n, L_{n+1}, and b as parameters, where R_n and L_n are the radius and half-length of the nth cell, respectively. Derivation of the matrix is presented in appendix A.

The transformation matrix from V_0 and i_0 to V_N and i_N defined by

$$\begin{pmatrix} V_N \\ i_N \end{pmatrix} = \begin{pmatrix} T_{11} & T_{12} \\ T_{21} & T_{22} \end{pmatrix} \begin{pmatrix} V_0 \\ i_0 \end{pmatrix} \tag{2}$$

is given by a product of the matrices $[t^{(n)}]$:

$$\begin{pmatrix} T_{11} & T_{12} \\ T_{21} & T_{22} \end{pmatrix} = \prod_{n=0}^{N-1} [t^{(n)}]. \tag{3}$$

If boundary conditions are imposed at the zeroth and Nth cell, the waveguide becomes a cavity with $(N+1)$ cells, and the resonant frequency of the cavity is given by a frequency f that satisfies one of the following equations.

$$T_{11} = 0 \quad \text{for} \quad i_0 = 0 \text{ (open)} \quad \text{and} \quad V_N = 0 \text{ (short)}, \tag{4}$$

$$T_{12} = 0 \quad \text{for} \quad V_0 = 0 \text{ (short)} \quad \text{and} \quad V_N = 0 \text{ (short)}, \tag{5}$$

$$T_{21} = 0 \quad \text{for} \quad i_0 = 0 \text{ (open)} \quad \text{and} \quad i_N = 0 \text{ (open)}, \tag{6}$$

$$T_{22} = 0 \quad \text{for} \quad V_0 = 0 \text{ (short)} \quad \text{and} \quad i_N = 0 \text{ (open)}. \tag{7}$$

Then, the values of V_n and i_n will be obtained from Eq. (1) as functions of V_0 or i_0, depending upon the boundary condition at the zeroth cell.

The Q-value of the $(N+1)$-cell cavity may be obtained as follows. Here, we assume that the field in each cell is TM010-like, and the power dissipation per one

period is very small compared with the stored energy (very high Q-value). Then, the stored energy U_n in the nth cell will be proportional to a volume v_n of the nth cell and a square of the current:

$$U_n \propto i_n^2 v_n. \tag{8}$$

Since the power dissipation P_n of the nth cell with the Q-value Q_n is given by

$$P_n = \omega U_n / Q_n, \tag{9}$$

the total Q-value Q_{tot} of the $(N+1)$-cell cavity becomes

$$Q_{\text{tot}} = \frac{\omega \sum_{n=0}^{N} U_n}{\sum_{n=0}^{N} P_n} = \frac{\sum_{n=0}^{N} U_n}{\sum_{n=0}^{N} U_n/Q_n} = \frac{\sum_{n=0}^{N} i_n^2 v_n}{\sum_{n=0}^{N} i_n^2 v_n/Q_n}. \tag{10}$$

The inverse of the total Q-value is an average of $1/Q_n$ weighted with the stored energy U_n.

3. APPLICATION OF THE DISK-LOADED WAVEGUIDE MODEL TO THE IDEALLY PERIODIC APS CAVITY

The APS cavity shown in Fig. 1 may be represented by a disk-loaded waveguide shown in Fig. 4, with appropriate boundary conditions. To distinguish an accelerating cell (a-cell) from a coupling cell (c-cell) a suffix *an* will be used for an accelerating cell and a suffix *cn* for a coupling cell. If the values of the parameters are the same for all of the accelerating cells, the cell number n in the suffix *an* is sometimes omitted. The same convention is also used for the coupling cells. To avoid confusion, it should be noted that an M-cell APS cavity comprises M *accelerating* cells.

An accelerating-cell frequency f_a is defined as the smallest eigenvalue of a π-mode boundary-condition problem of $i_c = 0$ and $V_a = 0$ (open at the c-cell and short at the a-cell) shown in Fig. 5a. This mode is sometimes referred to as an

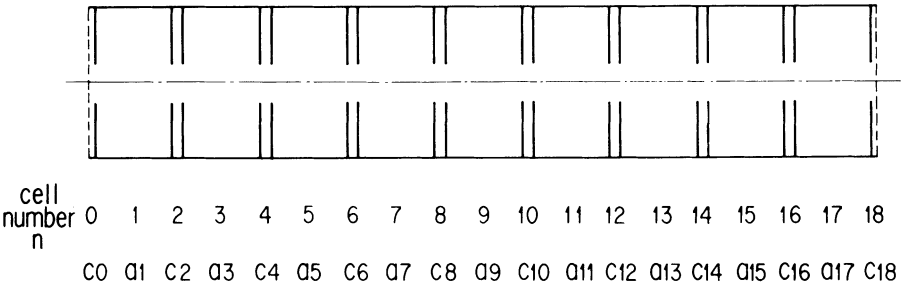

FIGURE 4 Disk-loaded waveguide terminated at the end coupling cells. This corresponds to the nine-cell APS cavity, if the open boundary condition is imposed at the end coupling cells.

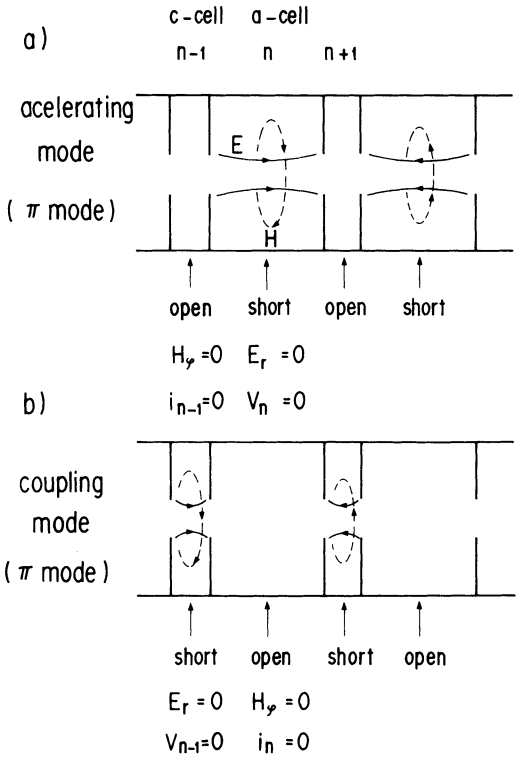

FIGURE 5 Accelerating and coupling modes of the disk-loaded waveguide.

accelerating mode. The boundary condition $V_a = 0$ implies that the electric field parallel to a boundary located at the center of the a-cell vanishes; that is, $E_r \propto V_a = 0$. On the other hand, the electric field normal to the boundary, that is, parallel to the beam direction, that will be used to accelerate the beam is induced by the azimuthal magnetic field $H_\phi \propto i_a$. The other boundary condition $i_c = 0$ indicates that the magnetic field vanishes on a boundary located at the center of the c-cell (the magnetic field normal to the boundary does not exist in the TM mode). The electric field is parallel to the boundary ($E_r \propto V_c$). Therefore, the accelerating mode that is like the TM010 mode in the accelerating cell becomes TM011-like in the coupling cell. Since the frequency of the TM011 mode in a pillbox cavity is very high compared with the TM010 mode, and the coupling through the beam aperture is very small compared with the difference, the field V_c is negligibly small in the coupling cell.

A coupling-cell frequency f_c is defined as the smallest eigenvalue of another π-mode boundary-condition problem of $V_c = 0$ and $i_a = 0$ (short at the c-cell and open at the a-cell) shown in Fig. 5b. This mode is sometimes referred to as a coupling mode.

The smallest and second-smallest eigenvalues of the boundary-condition problem of $V_c = 0$ and $V_a = 0$ (short at the c- and a-cell) are denoted by $f(0)$ and

$f(2\pi)$. Then, the width of the lowest passband of the ideally periodic APS waveguide is given by

$$\Delta f_{p1} = f_a - f(0) \quad \text{if} \quad f_a \leq f_c \tag{11}$$

or

$$\Delta f_{p1} = f_c - f(0) \quad \text{if} \quad f_a > f_c, \tag{12}$$

whereas the width of the second-lowest passband is given by

$$\Delta f_{p2} = f(2\pi) - f_c \quad \text{if} \quad f_a \leq f_c \tag{13}$$

or

$$\Delta f_{p2} = f(2\pi) - f_a \quad \text{if} \quad f_a > f_c. \tag{14}$$

The width of the stopband between the above two passbands becomes

$$\Delta f_s = |f_c - f_a|. \tag{15}$$

If the confluent condition of

$$f_a = f_c \tag{16}$$

is satisfied, the upper passband will join the lower passband, and the stopband will vanish. Then, the π mode will be located at the middle of the joined passband and obtain the finite group velocity.

The accelerating frequency of the TRISTAN main ring is

$$f_0 = 508.58 \text{ MHz}. \tag{17}$$

The resonant frequencies of the cavity shown in Fig. 1 were calculated using the computer program SUPERFISH, and values of parameters R_a and R_c were adjusted to make

$$f_a = f_c = f_0, \tag{18}$$

as listed in Table I, where the length of the coupling cell l_c was fixed at 15 mm. Then, the width of the joined passband Δf_p became

$$\Delta f_p / f_a = (\Delta f_{p1} + \Delta f_{p2}) / f_a = K = 1.0\%. \tag{19}$$

To simulate the cavity, values of the three parameters R_c, R_a, and b of the disk-loaded waveguide model shown in Fig. 2 and Fig. 3 were adjusted to reproduce the same values of f_a, f_c, and K as Eqs. (18) and (19). Here, values of $l_a = 2L_a$ and $l_c = 2L_c$ were fixed again. The values of the parameters thus obtained are also listed in Table I.

Then, the model was used to calculate various parameters of the ideally periodic nine-cell APS cavity shown in Fig. 4. The obtained dispersion curve and current distributions i_n among the cells are shown in Figs. 6 and 7, respectively. The open boundary condition of $i_0 = 0$ and $i_N = 0$ was imposed at the end coupling cells. In contrast to the waveguide, the 0 mode, 2π mode, and coupling mode are not allowed in the nine-cell APS cavity, since the imposed boundary condition is different from that of these modes. Thus, open circles are used to designate these virtual modes in the dispersion curve (Fig. 6).

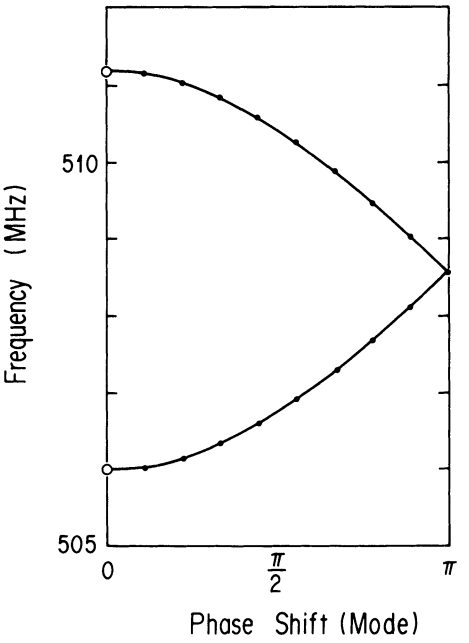

FIGURE 6 Dispersion curve of the disk-loaded waveguide. The $0\pi/9$ and $18\pi/9$ modes that are not allowed by the boundary conditions are designated by open circles. The confluent condition is satisfied in this dispersion curve.

It is seen from Fig. 7 that the current i_c in the coupling cell vanishes at the π mode, $f_a = f_0$ (accelerating mode). For the other modes, finite current flows in the coupling cell. Furthermore, it should be noted that the currents multiplied by the square roots of the lengths or the volumes of the cells are shown in the current distributions (Fig. 7), and those are well approximated by a sinusoidal function:

$$\sqrt{l_n} i_n \left(\frac{l\pi}{M} \text{mode} \right) \propto \sqrt{v_n} i_n \propto \sqrt{U_n}\, \text{sign}\,(i_n) \propto \sin \frac{l\pi}{N} \cdot n. \tag{20}$$

Here, sign (i_n) designates the sign of i_n. Since the volume or length of the coupling cell is by an order smaller than that of the accelerating cell, the maximum current or field in the coupling cell is larger, by an order of about a square root, than that in the accelerating cell except for the accelerating π mode. Further implications of Eq. (20) will be discussed in Section 6.

The distributions of i_n for the $(\pi + l\pi/M)$-mode can be obtained by reversing the signs of i_c of the coupling cells for the $(\pi - l\pi/M)$-mode, as seen by comparing the $10\pi/9$ mode with the $8\pi/9$ mode in Fig. 7. Thus, the distributions for the $11\pi/9$ to $17\pi/9$ modes are omitted in Fig. 7.

The Q-values of the accelerating and coupling modes were calculated with SUPERFISH as

$$Q_a = 43{,}830, \tag{21}$$

$$Q_c = 4{,}830. \tag{22}$$

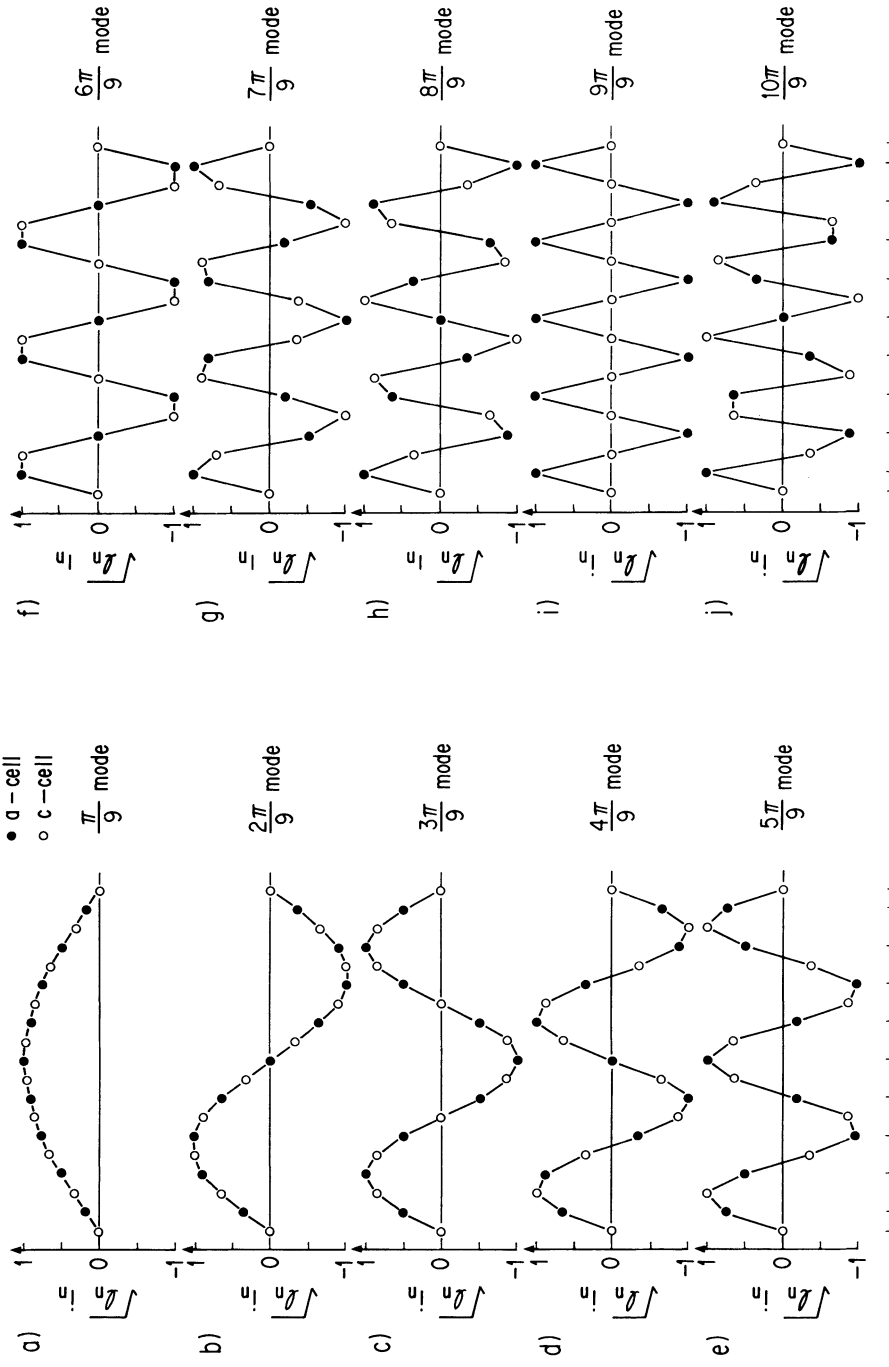

FIGURE 7 Current distributions among the cells. The currents in the accelerating cells are designated by solid circles, those in the coupling cells by open circles.

To improve the accuracy of the model calculation, the values of Eqs. (21) and (22) will be used in calculating total Q-values by Eq. (10). The Q-value of the TM010 mode of a pillbox cavity is approximately proportional to a ratio of the volume to the surface, and the ratio for the coupling cell is about ten percent of that for the accelerating cell. Thus, the Q-value Q_c of the coupling cell is about ten percent of Q_a. For the coupling mode, the power dissipation at the surface of the disk is a main contribution to the Q-value Q_c in the coupling cell.

The currents i_c in the coupling cell vanish for the π mode of the ideally periodic APS cavity. Then, the total Q-value of the π mode of the nine-cell cavity is simply the Q-value of the accelerating mode:

$$Q_{\text{tot}}(\text{ideal}) = Q_a, \tag{23}$$

as seen from Eq. (10) with $i_c = 0$. However, if the currents i_c in coupling cells increase for any reason, Q_c will contribute to the total Q-value in Eq. (10), and the total Q-value will decrease because $Q_c \ll Q_a$. In other words, the decrease of the Q-value will arise from the excitation of the coupling cells. Thus, the Q-values of modes other than the accelerating mode are much smaller than Q_a.

4. EFFECT OF DEVIATIONS FROM THE IDEAL PERIODICITY AND CONFLUENT CONDITION FOR A TWO-CELL APS CAVITY

In the preceding section the ideally periodic APS cavity was studied with the disk-loaded waveguide model. Henceforth we will investigate the effects of differences among accelerating-cell frequencies and the deviations of coupling-cell frequencies from the confluent condition. In this section the effects will be studied for the two-cell APS cavity shown in Fig. 8. In contrast to the preceding and next

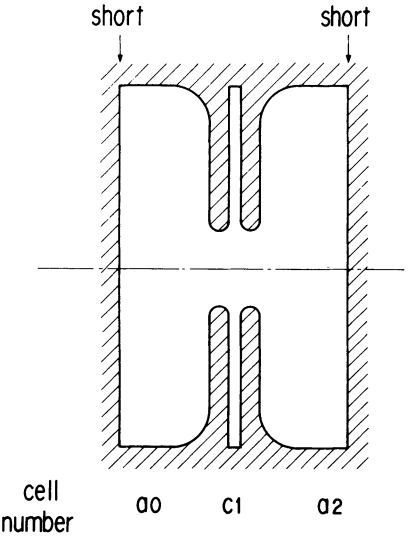

FIGURE 8 Two-cell APS cavity.

sections, the short boundary condition is imposed at the centers of the accelerating cells as $V_{a0} = V_{a2} = 0$. The values of f_{a0} and f_{c1} were fixed as

$$f_{a0} = f_0, \qquad f_{c1} = f_0 - 0.58\,\text{MHz}, \tag{24}$$

while the value of f_{a2} was varied:

$$\Delta f_{a2} = f_{a2} - f_0. \tag{25}$$

Effects of the variation of f_{a2} on the resonant frequency f_{res} and Q-value Q_{tot} were calculated with the model and SUPERFISH, and the results of the calculations are shown in Fig. 9.

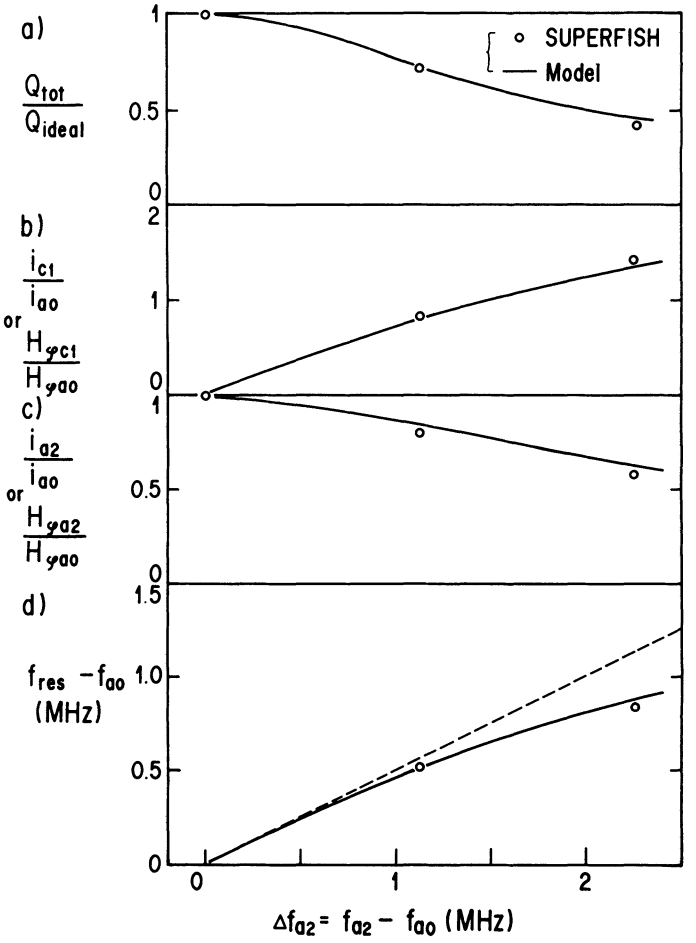

FIGURE 9 Results of the calculations by the model and SUPERFISH for the two-cell APS cavity. The solid curves show the results of the model calculation; the open circles show results of the SUPERFISH calculation. (a) Ratio of the Q-value to the ideal Q-value. (b) Ratio of the current or azimuthal magnetic field in the coupling cell ($c1$) to that in the $a0$ accelerating cell. (c) Ratio of the current or azimuthal magnetic field in the $a2$ accelerating cell to that in the $a0$-cell. (d) Variation of the resonant frequency f_{res} of the two-cell APS cavity versus $\Delta f_{a2} = f_{a2} - f_0$. The dotted line shows a line of $f_{\text{res}} = f_0 + \Delta f_{a2}/2$, that is, an average of the two accelerating-cell frequencies.

It is seen from Fig. 9a that the Q-value decreases as Δf_{a2} increases. The Q-value becomes about one-half of the ideal value at $\Delta f_{a2} \cong +2$ MHz. As mentioned in the preceding section, the decrease of the Q-value is presumed to arise from the excitation of the coupling cell. Figure 9b shows that a fairly strong field is excited in the coupling cell by increasing Δf_{a2}. The magnetic field $H_{\phi c1}$ or current i_{c1} is even higher than in the accelerating cell at $\Delta f_{a2} \cong +2$ MHz.

The increase of f_{a2} also has some effect on the field distribution among the accelerating cells. As seen from Fig. 9c, the magnetic field $H_{\phi a2}$ or current i_{a2} in the $a2$-cell decreases in comparison with $H_{\phi a0}$ or i_{a0} of the $a0$-cell, if f_{a2} deviates from f_{a0}. In other words, the power is distributed nonuniformly among the two accelerating cells.

Figure 9d shows that the resonant frequency of the two-cell APS cavity deviates from an average of the two accelerating-cell frequencies f_{a0} and f_{a2}; that is, $(f_{a0}+f_{a2})/2 = f_0 + \Delta f_{a2}/2$. This is a consequence of the nonuniform field distribution between the two accelerating cells and the excitation of the coupling cell.

In general an infinitesimal shift of a resonant frequency of a multicell cavity is given by an infinitesimal shift of an average of resonant frequencies of all cells weighted with the stored energies of the cells:

$$d(f_{\text{res}} - f_0) = d \frac{\sum_n U_n (f_n - f_0)}{\sum_n U_n} . \tag{26}$$

This equation is nothing but a perturbation theory[10] expressed in terms of stored energies. For the present case, the effect of Δf_{a2} on f_{res} is given by

$$f_{\text{res}} - f_0 = \int_0^{\Delta f_2} \frac{\frac{dU_1}{df_2}(f_1 - f_0) + U_2}{U_0 + U_1 + U_2} \cdot df_2, \tag{27}$$

where $dU_2/df_2(f_2 - f_0)$ is neglected. If U_2 were equal to U_0 and U_1 equal to zero, $f_{\text{res}} - f_0$ would be $\Delta f_2/2$. However, since the stored energy U_2 of the second a-cell becomes smaller than U_0, and the stored energy U_1 of the coupling cell with $f_1 - f_0 < 0$ appears as Δf_2 increases, the resonant frequency f_{res} deviates from $f_0 + \Delta f_2/2$.

Finally, it should be noted that the model calculation is in good agreement with the SUPERFISH calculation. Therefore, the disk-loaded waveguide model provides a useful means for studying the effect of the deviation from the ideal periodicity for the APS cavity. Slight difference between the two calculations should not be immediately attributed to a shortcoming of the model calculation; the accuracy of the calculation by the computer program SUPERFISH should also be examined.

5. EFFECT OF DEVIATIONS FROM THE IDEAL PERIODICITY AND CONFLUENT CONDITION FOR THE NINE-CELL APS CAVITY

In this section the effect of the deviations of f_{an} and f_{cn} from the resonant frequency f_{res} will be studied for the nine-cell APS cavity with the disk-loaded waveguide model. Practical design of the cavity will always be kept in mind, and, thus, this section will include some discussion about the design of the cavity.

The frequencies of four or five accelerating cells were set to $f_0 + |\Delta f_a|$, whereas those of the other accelerating cells were $f_0 - |\Delta f_a|$:

$$\begin{aligned} f_{an} &= f_0 + |\Delta f_a| \quad \text{for four or five } a\text{-cells} \\ f_{an} &= f_0 - |\Delta f_a| \quad \text{for the other } a\text{-cells.} \end{aligned} \tag{28}$$

It has been already found in the study of the two-cell APS cavity that the deviation of f_{an} from f_{res} should be of an order of 100 kHz to obtain 98 percent of the ideal Q-value. Thus, we first fixed the value of $|\Delta f_a|$ to 50 kHz.

As for the coupling-cell frequency, we will investigate three cases of

$$f_c = f_0, \qquad f_0 \pm 1\ \text{MHz}. \tag{29}$$

In the previous section we varied f_{a2} only, and, thus, both f_{c1} and f_{a2} deviated from f_{res}. As a result the effect of the deviation of f_{c1} from f_{res}, that is, the effect of the stopband, could not be clearly distinguished from that of the accelerating cell. In the present section, f_{an}'s are distributed as Eq. (28), keeping f_{res} equal to f_0 within about $|\Delta f_a|/9 \cong 6$ kHz, and, thus, the effect of the deviation of f_c from f_{res} can be studied independently of that of f_{an}.

The effect of the deviation of 1 MHz [Eq. (29)] should be studied for the following practical reason. If the high power is fed into the cavity, the cavity temperature will not be uniformly increased over that of its surface, since the power dissipation over the surface is not uniform. Then, thermal stress will be induced in the cavity body. Thermal-stress analysis indicates that the disks will be bent to the coupling cell in the case of the present design.[8] The bending of the disks increases the electric capacitance of the coupling cell and decreases f_c, while it decreases the capacitance of the accelerating cell and increases f_a. The effect of the bending on f_c is by about one order larger than that on f_{an}, since the length l_c of the coupling cell is about one-tenth of that of the accelerating cell. Furthermore, thermal expansion of the radius of the cavity lowers f_c, while it "overcancels" the above increase of f_{an}. In the case of the present design (150-kW input with the cooling water of 150 l/min), the decrease in f_c will amount to about 1 MHz, while the decrease of f_a will be about 0.1 MHz. For the accelerating cells, tuning plungers are necessary, in any event, to adjust the resonant frequency f_{res} to the accelerating frequency without the beam and to compensate for the beam-loading effect. For these purposes, it is not necessary to install tuners to the coupling cells. It is preferable to simplify a system by omitting the tuners for the coupling cells, if the 1-MHz deviation of f_c is allowable. Thus, effects of the 1-MHz stopband will be investigated.

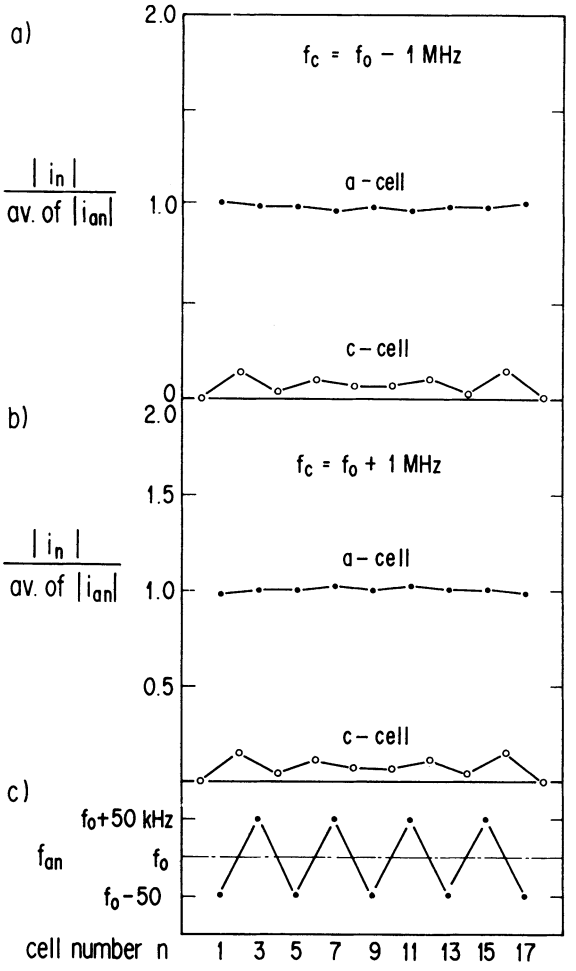

FIGURE 10 Field or current distributions among the cells in the cases of $f_c = f_0 \pm 1$ MHz. The currents in the accelerating cells are designated by solid circles, currents in the coupling cells by open circles. The currents are shown as ratios to the average current in the accelerating cells. The last figure (c) shows the distribution of the accelerating-cell frequencies.

At first we studied the case of

$$\begin{aligned} f_{a,2m-1} &= f_0 + 50\,\text{kHz} \quad (m \text{ even}) \\ f_{a,2m-1} &= f_0 - 50\,\text{kHz} \quad (m \text{ odd}); \end{aligned} \tag{31}$$

that is, f_{an} deviates from f_0 alternately as shown in Fig. 10c. This is similar to the case studied in the preceding section.

Results of the calculation are shown in Figs. 10 and 11. It is seen that the decrease of the Q-value is only 0.4 percent and independent of the value of f_c. On the other hand, the effect of the deviation of f_c from f_0 is observed in the field distribution among the accelerating cells. As mentioned in Section 3, the deviation of f_c induces the finite width of a stopband, giving rise to the

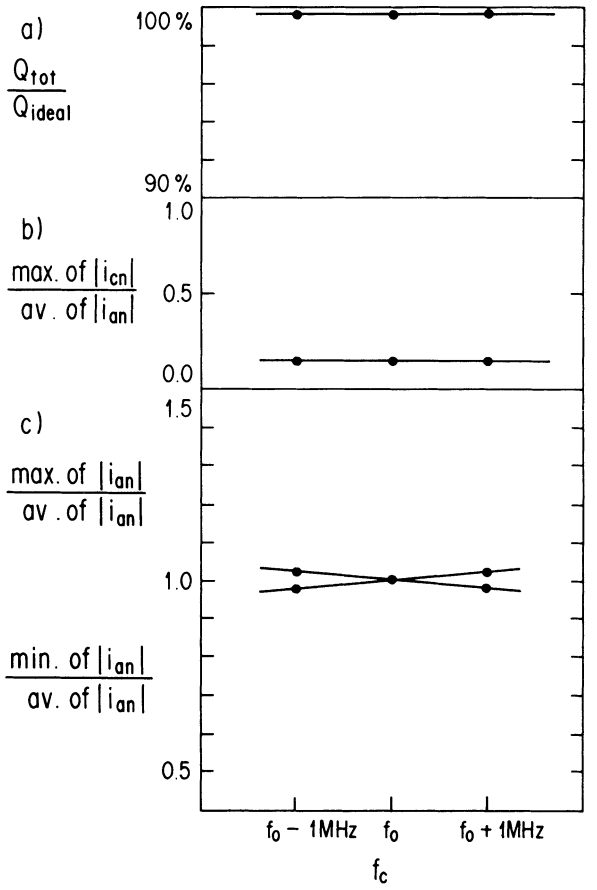

FIGURE 11 Dependences of the Q-value, maximum coupling-cell current, and maximum and minimum accelerating-cell currents on the coupling-mode frequency.

nonuniform field distribution among the accelerating cells. However, the difference between the maximum and minimum fields is only a few percent, even if the stopband width Δf_s amounts to 1 MHz, that is, of the same order as the passband width Δf_{p1}. Therefore, so far as the distribution of the deviations of f_{an} is like Eq. (31) or Fig. 10c, $|\Delta f_a| = 50$ kHz and $\Delta f_s = 1$ MHz will be allowable in view of the Q-value Q_{tot} and the field distribution.

While keeping the value of $|\Delta f_a| = 50$ kHz in Eq. (28) distributions of the deviations of f_{an} other than that expressed by Eq. (31) were explored. It turned out that the decrease of the Q-value is very dependent upon the distribution of the deviations, even if the value of $|\Delta f_a|$ is fixed. The worst distribution was the following:

$$\begin{aligned} f_{a,2m-1} &= f_0 + 50\text{ kHz} \quad (m \geq 5) \\ f_{a,2m-1} &= f_0 - 50\text{ kHz} \quad (m \leq 4), \end{aligned} \tag{32}$$

as shown in Fig. 12c. As seen from Fig. 13, the decrease of the Q-value amounts

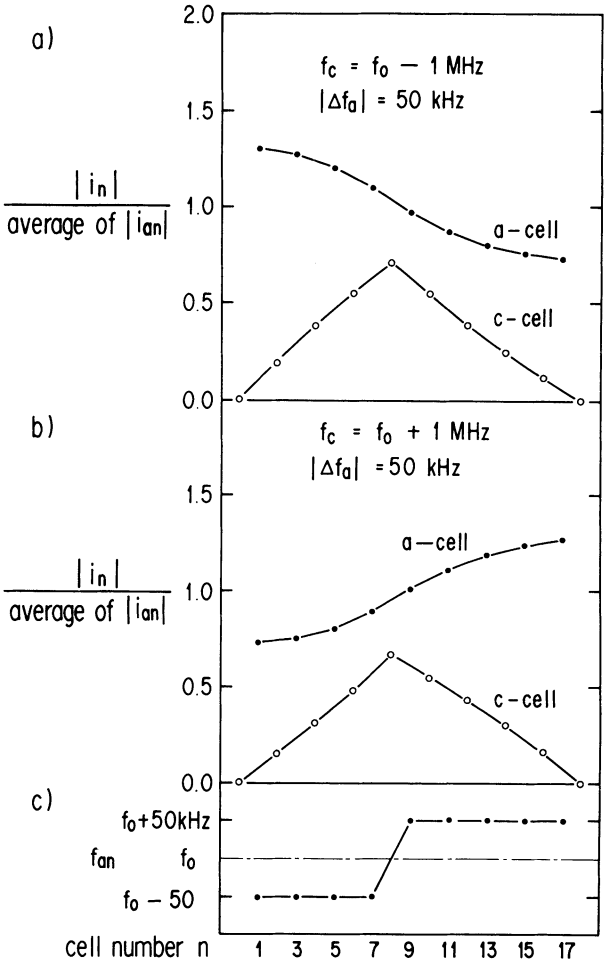

FIGURE 12 Field or current distributions among the cells in the cases of $f_c = f_0 \pm 1$ MHz. In contrast to Fig. 10(c), a different distribution of the accelerating frequencies is used, as shown in the last figure (c).

to about 8 percent. Also, the stopband of $\Delta f_s = 1$ MHz makes the maximum value of i_{an} 40 percent larger than the average value. It is seen from the field distribution shown in Fig. 12 that the field in the coupling cell is added from the end to the center cell, giving rise to the large excitation of the field in the center coupling cell.

Since the values of $|\Delta f_a| = 50$ kHz and $\Delta f_s = 1$ MHz cause too much degradation of the Q-value and too much nonuniformity of the field distribution among the accelerating cells, the cases of $|\Delta f_a| = 25$ kHz and $\Delta f_s = 0.5$ MHz were further studied. As seen from Fig. 13b, the excited field in the coupling cells is a linear function of $|\Delta f_a|$ but independent of the stopband width Δf_s. However, the maximum field of the accelerating cell divided by the average value is a linear function of both $|\Delta f_a|$ and Δf_s, as seen from Fig. 13c. Thus, Fig. 13 provides a

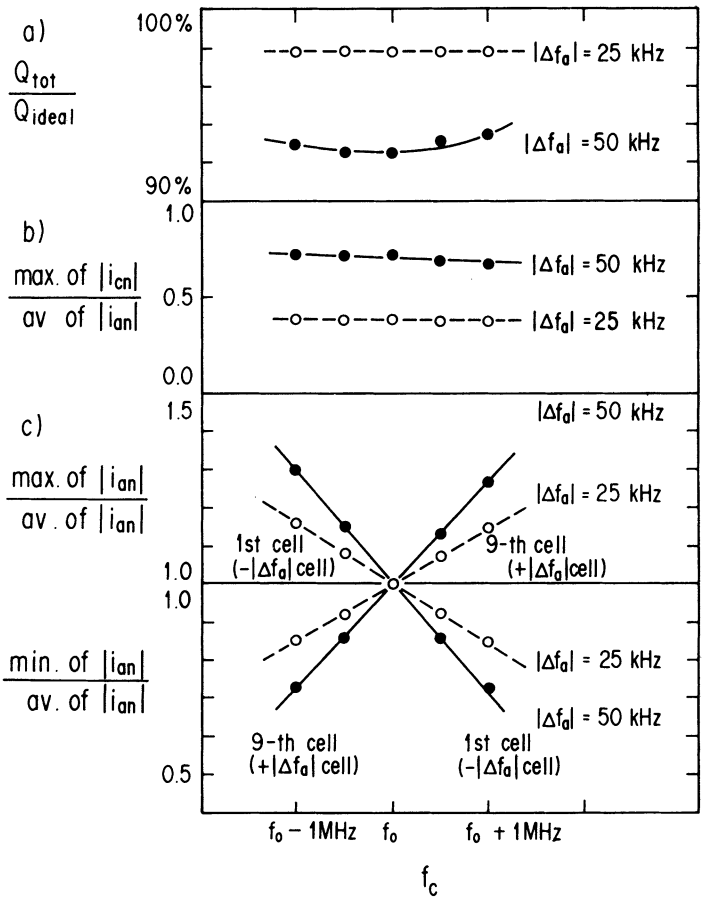

FIGURE 13 Dependence of the Q-value, maximum coupling-cell current, and maximum and minimum accelerating-cell current on the coupling-mode frequency.

means to determine the allowable values of $|\Delta f_a|$ and Δf_s from the necessary Q-value and the uniformity of the field distribution of the accelerating cells.

If the maximum deviation of f_{an} is within 10 kHz, the maximum field in the coupling cell will be less than 20 percent of the field in the accelerating cell, and the resulting decrease of the Q-value will be less than 1 percent. Even if the stopband width Δf_s is allowed to be 1 MHz, the field distribution among the accelerating cells will be uniform within 10 percent. If this Q-value and field distribution are allowed, the tuners will not be necessary for the coupling cells.

However, to realize the condition of $|\Delta f_a| < 10$ kHz, a tuner is necessary for each accelerating cell. Positions of the tuners can be adjusted to minimize the fields in the coupling cells, as described in Appendix B.

Although the adjustment is possible with the low-power measurement, it will be difficult during high-power operation and will require a sophisticated control system. Thus, we will set the positions of the tuners with the low-power measurement, and move them by the same amount during high-power operation.

The amount of the movement will be controlled to adjust the resonant frequency f_{res} of the nine-cell APS cavity to the accelerating frequency. Then, realization of $|\Delta f_a| < 10$ kHz will require a linearity of f_{an} to the tuner position. Also, the cooling system of each cell should be designed to obtain the same thermal shifts of f_{an} for all of the accelerating cells.

In this context it should be noted that more energy is stored in the low-frequency accelerating cells ($f_{an} < f_0$) than the high-frequency cells ($f_{an} > f_0$), if the coupling-mode frequency is lower than the resonant frequency ($f_c < f_0$), as seen from Figs 10a and 12a. However, if $f_c > f_0$, the distribution of the stored energies is reversed, as seen from Figs 10b and 12b. This property is important in view of the field stability for the following reason.

Suppose that the accelerating-cell frequency f_{an} is lowered by increasing the power dissipation P_{an}, as is usually the case. As the power is fed into the cavity, the lowering of f_{an} will be compensated by the motion of the tuner. However, since the tuner is moved by the same amount for all of the cells, this motion does not guarantee $f_{an} = f_{res}$ for all n. Then, f_{an} may become slightly lower than f_{res} for some reason. If the coupling-mode frequency f_c is lower than f_{res}, the condition of $f_{an} < f_{res}$ will increase the power dissipation P_{an} of the nth cell compared with the average. Then, the large power dissipation will further decrease f_{an}, resulting in the positive feedback condition, as seen from Fig. 14. Therefore, the coupling-mode frequency f_c should be always higher than, or equal to, the resonant frequency f_{res}.

It is fortunate that the APS cavity has this property, since one may set the coupling-mode frequency f_c to $f_0 + |\Delta f_{thermal}|$ at room temperature without the input power, where $\Delta f_{thermal}$ is the shift of f_c caused by the maximum input power. Then, as the power is increased, f_c will approach the confluent condition $f_c = f_0$, resulting in the more uniform field distribution and, thus, higher shunt impedance.

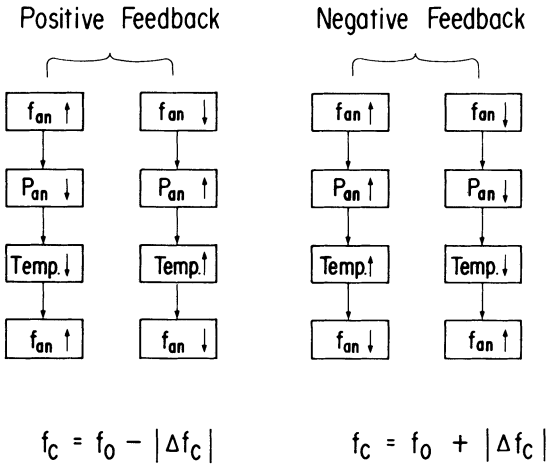

FIGURE 14 Feedback loop of the accelerating-mode frequency through the power dissipation and temperature.

6. DISCUSSION

In the preceding section the results of the calculation were discussed in view of the practical design of the nine-cell APS cavity. In this section the physical implications of the results will be further discussed, and an APS cavity with larger coupling cells will be proposed for the TRISTAN main ring.

The eigenmode in a cavity made of an ideally periodic disk-loaded waveguide with a very small iris is expressed in such a form that *the current multiplied by a square-root of the volume* is approximately a sinusoidal function of the cell number, as seen from Eq. (20). In other words, a characteristic variable is not a current i_n but $\sqrt{l_n}\, i_n$. This is quite different from the case of a large iris. If the iris is large, the disk acts as a small perturbator for an unloaded waveguide, and the power flows from one cell to another without a large reflection by the disk. Then, the eigenmode will be well approximated by that of the unloaded waveguide:

$$i_n\left(\frac{l\pi}{M}\,\text{mode}\right) \propto \sin\frac{l\pi}{N}n. \tag{33}$$

In this case *the current* is expressed as a sinusoidal function of the cell number.

However, if the iris is very small, almost all of the power is reflected by the disk, with a slight leak into the next cell, and the power will be reflected back by the disk on the other side of the cell. The reflections will be repeated many times, until the power is transferred from one cell to another. In other words, the electromagnetic energy is stored in each cell, while the power flows from one cell to another by a small leak of the power through the small iris. This picture implies that the characteristic variable is not a current but the square root of the stored energy, as expressed in Eq. (20).

It should be noted that this picture is not only valid for the accelerating cell but also for the coupling cell with the very small length of 15 mm. The coupling cell is geometrically different from the accelerating cell but electrically equivalent if $f_c = f_a$. The geometrical period of the APS cavity is a pair of an accelerating cell and a coupling cell, but the electrical period is one cell, whether it be an accelerating or coupling cell. Then, the accelerating mode defined geometrically as the π mode behaves electrically like the $\pi/2$ mode, guaranteeing a finite group velocity.

In modes other than the π mode the stored energy in a coupling cell is sometimes comparable to that in an accelerating cell. Then, the maximum field in the coupling cell becomes much higher than that in the accelerating cell, if the volume of the coupling cell is very small, as in the present case.

One may argue that the above discussion based upon the results of the model calculation cannot be applied to a real cavity with the very small coupling cells. It seems that a direct coupling between the accelerating cells is fairly strong, transferring most of the stored energy directly from one accelerating cell to another. However, the model calculation is in good agreement with the SUPERFISH calculation for the two-cell APS cavity, as seen in Section 4. This verifies the ability of the model to describe the characteristics of the real cavity.

If the periodicity is broken by letting the accelerating-cell frequencies deviate from f_0, the modes given by Eq. (20) are no longer eigenmodes but become mixed with each other. Figures 12, 7h, and 7j indicate that a frequency deviation like that shown in Fig. 12c gives rise to the field distribution approximated by

$$\sqrt{l_n}\, i_n \cong \sqrt{l_n}\, i_n\left(\frac{9}{9}\pi\right) - a\sqrt{l_n}\, i_n\left(\frac{8}{9}\pi\right) + b\sqrt{l_n}\, i_n\left(\frac{10}{9}\pi\right), \tag{34}$$

with small positive values of a and b, if the phase convention for i_n is taken as Fig. 7. The mixing of the $8\pi/9 = \pi - \pi/9$ and $10\pi/9 = \pi + \pi/9$ modes to the π mode arises from the perturbation, whose cell dependence includes a Fourier component mainly given by

$$\cos\frac{\pi}{9}m, \tag{35}$$

as seen from Fig. 12c. Here, $m = (n+1)/2$ is an accelerating-cell number. Since the frequency of the $9\pi/9$ mode is higher than that of the $8\pi/9$ mode and lower than that of the $10\pi/9$ mode, the sign of $(-a)$ is opposite to that of $(+b)$.

In the confluent case of $f_c = f_0$, the frequency difference between the $8\pi/9$ and π modes is similar to that between the π and $10\pi/9$ modes. Then, the value of a approaches that of b, and the second and third terms in Eq. (34) are canceled out in the accelerating cells. Consequently, the field distributions in the accelerating cells become uniform in the confluent case as is also expected from the finite group velocity, that is, vanishing of the stopband.

However, if f_c is higher than f_0, the π-mode frequency f_0 approaches that of the $8\pi/9$ mode, resulting in larger mixing of the $8\pi/9$ mode to the π mode. Thus, the deviations of the fields from the average in the accelerating cells become similar to the field distributions of the $8\pi/9$ mode (compare Fig. 12b with Fig. 7h). If f_c is lower than f_0, the $10\pi/9$ mode will be mixed with the π mode more than with the $8\pi/9$ mode, resulting in the field distribution shown in Fig. 12a.

The above discussion indicates that the APS cavity is advantageous only when the deviation from the confluent condition is small enough to allow cancellation of the second term by the third term in Eq. (34). Then, a figure of merit of the APS cavity will be given by a ratio

$$\Delta f_p / 2M\Delta f_s, \tag{36}$$

where the frequency difference between the π mode and $(M-1)\pi/M$ mode is approximated by $\Delta f_p/2M$. This is nothing but a ratio of half of the passband width to the stopband width, divided by the number of the cells, which may be easily obtained with some physical insight into the APS cavity.

In contrast to the field distributions among the accelerating cells, the excitation of the fields in the coupling cells and, thus, the Q-value are not dependent upon the value of f_c, as seen from Fig. 13b. In the coupling cells the second and third terms of Eq. (34) do not cancel but add, as seen by comparing the $8\pi/9$ mode with the $10\pi/9$ mode in Fig. 7, whatever the coupling-cell frequency. Thus, to keep the fields in the coupling cells from excitation, all of the accelerating-cell frequencies should be well tuned.

So far we have discussed the case of the deviation from the ideal periodicity given by Eq. (32) or Fig. 12c. If the deviation is like Eq. (31) or Fig. 10c, whose main Fourier component is

$$\cos \pi m, \tag{37}$$

the $\pi/9(\sim\pi - \pi)$ and $17\pi/9(\sim\pi + \pi)$ modes will be mainly mixed with the π mode. Since the frequency difference between the $\pi/9$ or $17\pi/9$ mode and the π mode is much larger than that between the $\pi \pm \pi/9$ and π modes, the effect of the deviation from the ideal periodicity becomes very small, as seen from Fig. 11.

Although the APS cavity was studied for the 15-mm length of the coupling cell, it is seen from the above discussion that the scaling for the other length is possible by interpreting the present results in terms of $\sqrt{l_n}\, i_n$ instead of i_n. Then, it is expected that a coupled-resonator model[3,4] with variables $\sqrt{l_n}\, i_n$ will provide another description of the APS cavity. An attempt was made to obtain essentially the same results as Fig. 13 with the coupled-resonator model, simplified by introducing some approximations, as shown in Appendix B. It turned out that one may summarize the results of the calculations as

$$\frac{\text{maximum of } \sqrt{v_c}\,|i_{cn}|}{\text{average of } \sqrt{v_a}\,|i_{an}|} \cong \frac{|\Delta f_a|}{\Delta f_p/2M} \tag{38}$$

and

$$\frac{|i_{a1}|}{\text{average of } |i_{an}|} \cong 1 + \frac{1}{2}\frac{\Delta f_c}{\Delta f_p/2M} \cdot \frac{\Delta f_a}{\Delta f_p/2M}, \tag{39}$$

where $\Delta f_c = f_c - f_{\text{res}}$ ($\Delta f_s = |\Delta f_c|$) and $\Delta f_a = f_{a1} - f_{\text{res}}$.

Finally, it is noted that the problem of the APS cavity found in the present study can be eased by increasing the volume or length of the coupling cell. Suppose that the length of the coupling cell is doubled to $l_c = 30$ mm. The stored energy or $\sqrt{l_n}\, i_n$ leaked into the coupling cell is the same as the case of $l_c = 15$ mm. However, the Q-value of the coupling mode is doubled, since the volume is doubled but the surface remains approximately the same. Then, the decrease of the Q-value due to the deviation from the ideal periodicity will be reduced to half, as seen from Eq. (10). Furthermore, the field in the coupling cell will be lowered by a factor of $\sqrt{2}$, since $\sqrt{l_c}\, i_c$ is the same, and l_c is doubled.

The other advantage is that the effect of the bending of the disks on the resonant frequency is halved by doubling the length of the cell. Since the decrease $\Delta f_{\text{thermal}}$ of the coupling-cell frequency f_c due to the power input is reduced to half, the stopband width $\Delta f_s = \Delta f_{\text{thermal}}$ at room temperature without the power input becomes small, resulting in a more uniform field distribution among the accelerating cells. It is also noted that allowable machining and welding errors for the bending of the disks are doubled.

The disadvantage of increasing the length l_c of the coupling cell is that the shunt impedance of the APS cavity becomes smaller. The shunt impedance for $l_c = 30$ mm calculated by the SUPERFISH is compared with that for $l_c = 15$ mm in Table I. It is seen that the decrease of the ideal shunt impedance is only 2

percent. Consequently, we propose the 30-mm length of the coupling cell for the TRISTAN main ring.

7. CONCLUSION

The results of the calculation by the disk-loaded waveguide model with a proper parametrization are in good agreement with those by SUPERFISH for the two-cell APS cavity. Thus, the model provides a useful means to study a multicell APS cavity. In the ideally periodic APS cavity, the eigenmodes are expressed in such a form that $\sqrt{l_n}\, i_n$ is approximately a sinusoidal function of the cell number n.

If the peridocity is slightly broken by introducing the differences of the accelerating-cell frequencies as $f_{an} = f_0 \pm |\Delta f_a|$ with a constraint of $f_{\text{res}} \cong f_0$, then the fields are excited in the coupling cells, resulting in a decrease of the Q-value. The excitation is strongest if the distribution of the deviations of f_{an} from f_0 is like $f_{a,2m-1} - f_0 \cong |\Delta f_a| \cos \pi m/M$. The maximum field or current in the coupling cells is well approximated by Eq. (38).

If the stopband appears by allowing the coupling-cell frequency f_c to deviate from the resonant frequency f_{res} ($\Delta f_s = |f_c - f_{\text{res}}|$), then the stored energy is distributed nonuniformly among the accelerating cells. A ratio of the maximum to the average current is given approximately by

$$\frac{\text{max. of } |i_{an}|}{\text{av. of } |i_{an}|} \cong 1 + \frac{1}{2}\frac{\Delta f_s}{\Delta f_p/2M} \cdot \frac{|\Delta f_a|}{\Delta f_p/2M}. \tag{40}$$

To stabilize the field distribution among the accelerating cells, the coupling-mode frequency should be set higher than, or equal to, the accelerating-mode frequency, if the accelerating-mode frequency is lowered by feeding power into the cavity.

REFERENCES

1. T. Nishikawa, S. Giordano, and D. Carter, *Rev. Sci. Instrum.* **37,** 652 (1966).
2. T. Kikuchi and K. Takata, *Jpn. J. Appl. Phys.* **9,** 679 (1970).
3. D. E. Nagle, E. A. Knapp, and B. C. Knapp, *Rev. Sci. Instrum.* **38,** 1583 (1967).
4. E. A. Knapp, B. C. Knapp, and J. M. Potter, *Rev. Sci. Instrum.* **39,** 979 (1968).
5. J. McKeown and S. O. Schriber, *IEEE Trans. Nucl. Sci.* **NS-28,** 2755 (1981).
6. H. Herminghaus *et al.*, *IEEE Trans. Nucl. Sci.* **NS-30,** 3274 (1983).
7. T. Higo, S. Inagaki, Y. Yamazaki, and K. Takata, *Proc. 5th Symp. Accel. Sci. Tech.* (Tsukuba, 1984, p. 114).
8. T. Higo, Y. Yamazaki, T. Kageyama, M. Akemoto, H. Mizuno, and K. Takata, *IEEE Trans. Nucl. Sci.* **NS-32,** 2834 (1985).
9. K. Halbach and R. F. Holsinger, *Particle Accelerators* **7,** 213 (1976).
10. J. C. Slater, *Microwave Electronics,* (D. Van Nostrand, New York, 1950).

APPENDIX A

Derivation of the Transformation Matrix $[t^{(n)}]$

The transformation matrix $[t^{(n)}]$ is derived in this appendix. Denote characteristic impedance, admittance, and propagation constant in vacuum by Z_0, Y_0, and β_0, respectively. If the radius of the nth cell is R_n, then the cutoff frequency is given by

$$f_{\text{cut},n} = j_{01}c/2\pi R_n, \tag{A-1}$$

where j_{01} is the first zero point of the 0th order Bessel function. If half of a length of the nth cell is L_n, then the phase advance ϕ_n from the center of the nth cell to the iris is given by

$$\phi_n = \alpha_n \beta_0 L_n, \tag{A-2}$$

where α_n for the frequency f is defined as

$$\alpha_n^2 = 1 - (f_{\text{cut},n}/f)^2. \tag{A-3}$$

Using the characteristic impedance Z_n of the waveguide:

$$Z_n = \alpha_n Z_0, \tag{A-4}$$

the voltage V_n and current i_n at the center of the nth cell are expressed as

$$V_n = V^+ + V^- \tag{A-5}$$

and

$$Z_n i_n = V^+ - V^-, \tag{A-6}$$

respectively, whereas those at the iris on the nth cell side as

$$V'_n = V^+ e^{-j\phi} n + V^- e^{j\phi} n \tag{A-7}$$

and

$$Z_n i'_n = V^+ e^{-j\phi} n - V^- e^{j\phi} n, \tag{A-8}$$

respectively. Here, V^+ and V^- are voltages of traveling waves from left to right and from right to left, respectively, in Fig. 3. Eliminating V^+ and V^- in Eqs. (A-5) to (A-8) we obtain

$$\begin{pmatrix} V'_n \\ i'_n \end{pmatrix} = \begin{pmatrix} C_n & -jZ_0\alpha_n S_n \\ -jY_0 \dfrac{1}{\alpha_n} S_n & C_n \end{pmatrix} \begin{pmatrix} V_n \\ i_n \end{pmatrix}, \tag{A-9}$$

where we use notations

$$C_n = \cos\phi_n, \qquad S_n = \sin\phi_n \tag{A-10}$$

for simplicity.

The voltage V'_{n+1} and current i'_{n+1} at the iris on the $(n+1)$th cell side are given

by

$$V'_{n+1} = V'_n, \qquad i'_{n+1} = i'_n - jbY_0 V'_n, \tag{A-11}$$

that is,

$$\begin{pmatrix} V'_{n+1} \\ i'_{n+1} \end{pmatrix} = \begin{pmatrix} 1 & 0 \\ -jbY_0 & 1 \end{pmatrix} \begin{pmatrix} V'_n \\ i'_n \end{pmatrix}. \tag{A-12}$$

Then, the transformation matrix $[t^{(n)}]$ is obtained by multiplying Eq. (A-9) times Eq. (A-12) and Eq. (A-9) for $n+1$:

$$\alpha_n t_{11}^{(n)} = \alpha_n C_{n+1} C_n - \alpha_{n+1} S_{n+1} S_n - b\alpha_{n+1}\alpha_n S_{n+1} C_n \tag{A-13}$$

$$\alpha_{n+1} t_{22}^{(n)} = \alpha_{n+1} C_{n+1} C_n - \alpha_n S_{n+1} S_n - b\alpha_{n+1}\alpha_n C_{n+1} S_n \tag{A-14}$$

$$jY_0 t_{12}^{(n)} = \alpha_n C_{n+1} S_n + \alpha_{n+1} S_{n+1} C_n - b\alpha_{n+1}\alpha_n S_{n+1} S_n \tag{A-15}$$

$$jZ_0\alpha_{n+1}\alpha_n t_{21}^{(n)} = \alpha_{n+1} C_{n+1} S_n + \alpha_n S_{n+1} C_n + b\alpha_{n+1}\alpha_n C_{n+1} C_n. \tag{A-16}$$

Note that $t_{11}^{(n)}$ and $t_{22}^{(n)}$ are always real, whereas $t_{12}^{(n)}$ and $t_{21}^{(n)}$ are always imaginary, even if the frequency f is lower than the cutoff frequency. (If $f < f_{\mathrm{cut},n}$, then α_n and S_n are both imaginary.)

APPENDIX B

Coupled Oscillators and a Method for Tuning The Accelerating Cells

A system of coupled oscillators is expressed in the form

$$\frac{d^2x}{dt^2} + \omega_n^2 x_n = \sum_l K_{nl} x_l. \tag{B-1}$$

This equation stands for various physical systems. It is possible to write an equivalent circuit for a physical system that can be described by Eq. (B-1). Then, Eq. (B-1) may be referred to as a coupled resonator model.[3,4] Problems are what physical quantities are represented by the variables x_n and coupling parameters K_{nl}. The discussion in Section 5 led us to an attempt of

$$x_n \propto \sqrt{l_n}\, i_n \propto \sqrt{v_n}\, i_n \tag{B-2}$$

and

$$K_{nl} = \tfrac{1}{2} K \omega_n^2 \delta_{l,n\pm1} \tag{B-3}$$

for the APS cavity, even if the length of the coupling cell is very small compared with that of the accelerating cell. The parameter K in Eq. (B-3) is equivalent to that defined by Eq. (19), as will be shown later.

If the time variation of x_n is given by $e^{j\omega t}$, and if the approximation

$$\frac{|\omega - \omega_n|}{\omega_n} \ll 1 \tag{B-4}$$

is justified, then Eq. (B-1), with Eq. (B-3), becomes

$$\frac{4\Delta f_n}{\Delta f_p} x_n = x_{n-1} + x_{n+1}, \tag{B-5}$$

where Δf_p is defined by Eq. (19) as $\Delta f_p = K f_n$ ($\omega_n = 2\pi f_n$, $\omega = 2\pi f$). Also, we denote

$$\Delta f_n = f_n - f. \tag{B-6}$$

To distinguish the a-cell from the c-cell we rewrite Eq. (B-5) as

$$\frac{4\Delta f_{c,2m}}{\Delta f_p} x_{c,2m} = x_{a,2m-1} + x_{a,2m+1} \tag{B-7}$$

$$\frac{4\Delta f_{a,2m-1}}{\Delta f_p} x_{a,2m-1} = x_{c,2m-2} + x_{c,2m}. \tag{B-8}$$

When $f_{a,2m-1} = f_a$ for any m, one of solutions of Eqs (B-7) and (B-8) is given by $f = f_a$, $x_{c,2m} = 0$, and $x_{a,2m-1} = -x_{a,2m+1}$ ($\neq 0$) for any m. This is the accelerating π mode, and, thus, f_a is the accelerating-mode frequency. When $f_{c,2m} = f_c$ for any m, one of solutions is given by $f = f_c$, $x_{a,2m-1} = 0$, and $x_{c,2m-2} = -x_{c,2m}$ ($\neq 0$) for any m. This is the coupling π mode, and, thus, f_c is the coupling-mode frequency. Finally, when $f_n = f_0$ for any n, we obtain $x_{n-1} = x_n$ for any n with $f = f_0 - \Delta f_p/2$ or $x_{n-1} = -x_n$ for any n with $f = f_0 + \Delta f_p/2$. The former is the 0 mode, whereas the latter is the 2π mode. Since Δf_p becomes the width of the joined passband, the parameter K in Eq. (B-3) is equivalent to that of Eq. (19).

Henceforth we consider the M-cell APS cavity while imposing the boundary condition of

$$x_{c0} = x_{c,2M} = 0. \tag{B-9}$$

We concentrate on the accelerating π mode of

$$x_{a,2m-1} = (-)^{m-1} \text{ sign } (x_{a1}) \, |x_{a,2m-1}| \tag{B-10}$$

and study the effect of the differences among the accelerating cell frequencies $f_{a,2m-1}$. However, by equating all of $\Delta f_{c,2m}$'s to the same value Δf_c

$$\Delta f_{c,2m} = \Delta f_c \quad \text{for any } m, \tag{B-11}$$

the effect of the stopband width

$$\Delta f_s = |\Delta f_c| \tag{B-12}$$

will be investigated. Then, Eqs (B-7) and (B-8) can be written as

$$|x_{a,2m+1}| - |x_{a,2m-1}| = (-)^m \text{ sign } (x_{a1}) \frac{4\Delta f_c}{\Delta f_p} x_{c,2m} \tag{B-13}$$

and

$$(-)^{m-1}(x_{c,2m} + x_{c,2m-2}) = \text{sign } (x_{a1}) \cdot \frac{4\Delta f_{a,2m-1}}{\Delta f_p} |x_{a,2m-1}|. \tag{B-14}$$

If the stopband vanishes as $\Delta f_c = 0$, we obtain $|x_{a,2m+1}| = |x_{a,2m-1}|$ from Eq. (B-13), and, thus, the currents i_{an} are distributed uniformly among the accelerating cells regardless of the accelerating-mode frequencies. However, the fields in the coupling cells are excited, if $\Delta f_{a,2m-1} \neq 0$, since $|x_{c,2m}| \neq |x_{c,2m-2}|$ is obtained from Eq. (B-14), and, then, at least $|x_{c2}| \neq |x_{c0}| = 0$. The fields in the coupling cells vanish only in the case of $\Delta f_{a,2m-1} = 0$ for any m, since $|x_{c,2m}| = |x_{c,2m-2}| = 0$ is derived from Eqs (B-14) and (B-9).

Summing up Eq. (B-14) for $m = 1$ to m gives

$$x_{c,2m} = (-)^{m-1} \operatorname{sign}(x_{a1}) \sum_{l=1}^{m} \frac{4\Delta f_{a,2l-1}}{\Delta f_p} |x_{a,2l-1}|. \tag{B-15}$$

Also, summing up Eq. (B-13) for $m = 1$ to $m - 1$ and substituting Eq. (B-15) give

$$|x_{a,2m-1}| - |x_{a1}| = -16 \frac{\Delta f_c}{\Delta f_p} \sum_{l=1}^{m-1} \sum_{k=1}^{l} \frac{\Delta f_{a,2k-1}}{\Delta f_p} |x_{a,2k-1}|. \tag{B-16}$$

It is seen from Eq. (B-15) that the maximum excitation of the coupling cells occurs when

$$\Delta f_{a,2m-1} = \Delta f_a \quad \text{for } 1 \leq m \lesssim M/2 \tag{B-17}$$

and

$$\Delta f_{a,2m-1} = -\Delta f_a \quad \text{for } M/2 \lesssim m < M. \tag{B-18}$$

By approximating $|x_{a,2k-1}|$ by an average $|x_a|$ in the right-hand sides of Eqs (B-15) and (B-16), we obtain

$$\frac{|x_{cM}|}{|x_a|} \simeq \frac{|\Delta f_a|}{\Delta f_p/2M} \tag{B-19}$$

and

$$\frac{|x_{a1}|}{|x_a|} \simeq 1 + \frac{1}{2} \frac{\Delta f_c}{\Delta f_p/2M} \cdot \frac{\Delta f_a}{\Delta f_p/2M}, \tag{B-20}$$

where the approximation of $M \gg 1$ is also used. Note that $|x_{a,M-1}| \cong |x_a|$ in the left-hand side of Eq. (B-16). It is seen from Eq. (B-20) that $|x_{a1}| > |x_a|$ if $\Delta f_c > 0$ and $\Delta f_a > 0$. Thereby all the essential properties of the APS cavity can be derived from Eqs (B-7) and (B-8), if the variables x_n are chosen as $x_n = \sqrt{l_n}\, i_n$.

Equation (B-8) suggests a simple method for tuning each of the accelerating cells to a resonant frequency. First, the tuners of the a-cells are moved to approximately match the confluent condition. Then, $|x_{a,2m-1}|$ becomes $|x_a|$ for all m. Also, a signal $y_{c,2m}$ from a coupling probe is detected at each of the coupling cells, where $y_{c,2m} = Ax_{c,2m}$ with a constant A. If the dependence of the accelerating-cell frequency on the tuner position d_{2m-1} is given by $\Delta f_{a,2m-1} = C\Delta d_{2m-1}$, then Eq. (B-8) becomes

$$\Delta d_1 = By_{c2} \tag{B-21}$$

and

$$\Delta d_{2m-1} = (-)^{m-1} B(y_{c,2m-2} + y_{c,2m}), \tag{B-22}$$

where $B = \text{sign}\,(x_{a1})\, A\Delta f_p/(4C\,|x_a|)$. The constant B can be obtained as follows. Adjust the tuner of the first accelerating cell to eliminate y_{c2}. If the displacement of the tuner is D, one obtains the calibration constant B as

$$B = \frac{M-1}{M}\frac{D}{y_{c2}}, \tag{B-23}$$

where the shift of the resonant frequency due to the displacement D is approximated by CD/M.

Since the calibration constant B is known from Eq. (B-23), we can determine the displacement Δd_{2m-1} from Eq. (B-22) by measuring the signals $y_{c,2m}$. It should be noted that it is necessary to know not only the amplitude but also the phase of $y_{c,2m}$, at least relative to y_{c2}. Also, Eq. (B-22) is based upon the approximation of Eq. (B-4), and, thus, an iteration may be necessary if the initial positions of the tuners are far from the final positions. However, the convergence will be very fast, since the approximation becomes better as the iteration proceeds.